# A DIFFERENTIAL ALGEBRAIC MODEL FOR THE SIMULATION OF THERMOSIPHON SYSTEMS

Santos M.P., Lima E.R.A. and Costa A.L.H*.
*Author for correspondence
Chemical Engineering Postgraduate Program
Rio de Janeiro State University (UERJ),
Rio de Janeiro
Brazil,
E-mail: andrehc@uerj.br

## ABSTRACT

The main alternative employed for the reboiler in distillation towers is the thermosiphon. In this case, the flow circulation does not depend on the existence of a pump, the flow is promoted by the difference in the density between the liquid column inside the distillation tower and the two-phase stream along the heat exchanger. Despite its importance, few papers have presented a full analysis of the simulation of this kind of system. In this context, this work discusses a differential algebraic model for the simulation of vertical thermosiphons. The model describes the behaviour of the entire hydraulic system, encompassing the feed piping, the heat exchanger and the return pipe to the column. The model is composed of mass, momentum and energy balances. The vaporizing stream can be composed of any number of components. Transport parameters for each phase are evaluated using proper correlations. The resultant mathematical model is composed of a set of differential algebraic equations. The application of the proposed approach is illustrated using a typical reboiler example.

## INTRODUCTION

Reboilers are heat exchangers responsible for providing energy to the fractionation process in distillation columns, one of the unit operations most used in the chemical industry. As a result, this work presents the modelling and simulation of vertical thermosiphons. In this kind of reboiler, the circulation occurs due to the density difference between the column of liquid in the bottom of the distillation tower and the two-phase stream returning to the tower [1]. Commonly, boiling occurs in the tube side (shell side boiling in vertical termosiphons are only adopted in special cases, e.g. heating using a corrosive stream [2]).

Comparing with forced flow reboilers, thermosiphons have the advantage to do not present operational costs, because there is no recirculation pump. In relation to kettle reboilers, thermosiphons are less prone to fouling and demands lower capital costs. In terms of its orientation, vertical thermosiphons are more compact and are associated to higher convective heat transfer coefficients than horizontal thermosiphons. However, vertical thermosiphons may be very sensitive to operation conditions, due to the nature of natural flow [3].

## NOMENCLATURE

| | | |
|---|---|---|
| $Cp$ | [J/kg K] | Heat capacity |
| $De$ | [m] | Outer tube diameter |
| $Di$ | [m] | Inner tube diameter |
| $F$ | [-] | Enhancement factor |
| $f$ | [-] | Friction factor |
| $g$ | [m/s²] | Gravity acceleration |
| $G$ | [kg/ m² s] | Mass flux |
| $H$ | [W] | Enthalpy rate |
| $hcb$ | [W/m² K] | Convective boiling heat transfer coefficient |
| $he$ | [W/m² K] | Shell-side convective heat transfer coefficient |
| $H^E$ | [J/mol] | Molar excess enthalpy |
| $hi$ | [W/m² K] | Tube-side convective heat transfer coefficient |
| $hl$ | [W/m² K] | Heat transfer coefficient for liquid flowing alone |
| $hnb$ | [W/m² K] | Heat transfer coefficient in nucleate boiling |
| $k$ | [W/m K] | Thermal conductivity |
| $kw$ | [W/m K] | Thermal conductivity of the tube wall |
| $L$ | [m] | Length of tube |
| $mL$ | [kg/s] | Liquid mass flow rate |
| $MMmg$ | [kg/mol] | Molar mass of the gas mixture |
| $MMml$ | [kg/mol] | Molar mass of the liquid mixture |
| $mT$ | [kg/s] | Total mass flow rate |
| $mV$ | [kg/s] | Vapour mass flow rate |
| $Ntt$ | [-] | Total number of tubes |
| $P$ | [Pa] | Pressure |
| $Pr$ | [-] | Prandtl number |
| $q''$ | [W/m] | Heat flux |
| $Rfe$ | [m²K/W] | Shell-side fouling resistance |
| $Rfi$ | [m²K/W] | Tube-side fouling resistance |
| $T$ | [K] | Temperature |
| $T_H$ | [K] | Hot stream temperature |
| $Tsat$ | [K] | Saturation temperature |
| $Tw$ | [K] | Wall temperature |
| $Twonb$ | [K] | Onset nucleate boiling temperature |
| $U$ | [W/m² K] | Overall heat transfer coefficient |
| $x$ | [-] | Molar fraction of the liquid phase |
| $Xtt$ | [-] | Lockhart- Martinelli parameter for turbulent flow |
| $y$ | [-] | Molar fraction of the vapor phase |
| $\Delta H^V$ | [J/mol] | Latent heat of vaporization |
| $\theta$ | [-] | Angle |
| $\rho$ | [kg/m³] | Density |
| $\rho_{tp}$ | [kg/m³] | Two-phase density |
| $\Sigma$ | [N/m] | Surface tension |
| $\varphi_{lo}^2$ | [-] | Two-phase pressure drop enhancement factor |
| $\mathcal{V}$ | [-] | Molar vaporized fraction |

## SYSTEM

The thermosiphon system is illustrated in Figure 1. The flow circuit is organized in four regions.

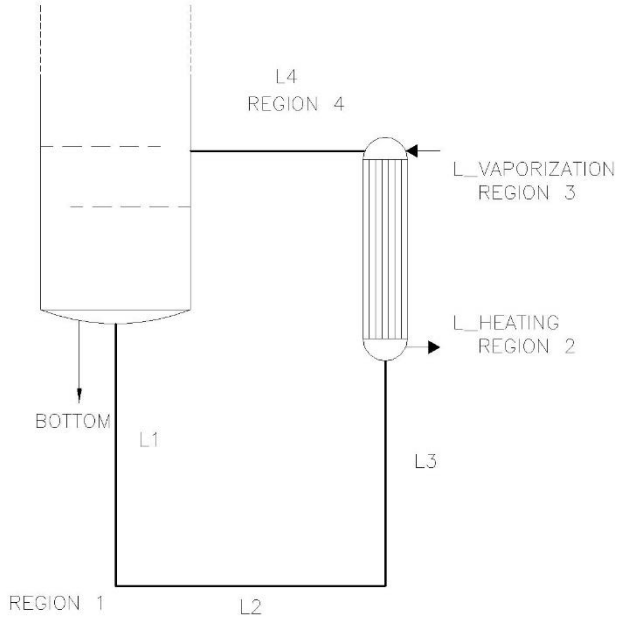


**Figure 1** Schematic representation of the system

In Region 1, the liquid stream flows from the bottom of the tower to the heat exchanger inlet. Region 2 encompasses the heat exchanger flow without bulk phase change until reach saturated conditions. Region 3 encompasses the heat exchanger saturated boiling. Region 4 consists in the two-phase flow from the heat exchanger outlet to the column bottom.

## MODELING

The system model is composed of energy, momentum and mass balances.

The energy balance in the heat exchanger is given by:

$$\frac{dH}{dL} = Ntt\ \pi DeU(T_H - T) \tag{1}$$

where the overall heat transfer coefficient (*U*) is represented by [4]:

$$U = \frac{1}{\left(\frac{De}{Di}\right)\left(\frac{1}{hi}\right)+\left(\frac{De}{Di}\right)Rfi+\frac{De\ ln(De/Di)}{2\ kw}+Rfe+\left(\frac{1}{he}\right)} \tag{2}$$

The convective heat transfer coefficient in the boiling region is calculated using two contributions: convective boiling (*hcb*) and nucleate boiling (*hnb*).

The contribution of convective boiling is calculated by the multiplication of the forced convection coefficient of the liquid flow (*hl*) by an amplification factor (*F*), a function of the Lockhart-Martinelli parameter (*Xtt*). This contribution is associated with the intensification of forced convection due to the phase change.

The contribution of nucleate boiling is directly linked to the bubble formation, calculated according to Palen [3]. Nucleate boiling occurs if the wall temperature (*Tw*) is larger than the onset nucleate boiling temperature (*Twonb*).

The model equation that describes the wall temperature is:

$$\frac{T_H - T_w}{\frac{1}{h_e De}+\frac{R_{f,e}}{De}+\frac{ln\left(\frac{De}{Di}\right)}{2k_w}+\frac{R_{f,i}}{Di}} = \frac{T_w - T}{\frac{1}{h_i Di}} \tag{3}$$

The onset nucleate boiling is calculated using the following correlation [5]:

$$T_{wonb} = T_{sat} + \left(\frac{8\sigma q" T_{sat}}{k_l \Delta H^V \rho_g}\right)^{\frac{1}{2}} Pr_l \tag{4}$$

The enthalpy rate in the energy balance is related to the temperature and pressure by [6]:

$$H = \left(\int_{T_{ref}}^{T} \sum_{j=1}^{n} x_j Cp_{l_j}(T)dT + \frac{H^E(T,x)}{MMml}\right) mL + \left(\frac{\sum_{j=1}^{n} y_j \Delta H_j^{vap}(T_{ref})}{MMmg} + \int_{T_{ref}}^{T} \sum_{j=1}^{n} y_j Cp_j^{g.i.}(T)dT\right) mV \tag{5}$$

The mechanical energy for the single-phase flow is represented by:

$$-\frac{dP}{dL} = -\frac{G^2}{\rho^2}\frac{d\rho}{dL} + \rho\ g\ sen\theta + \frac{f\ G^2}{2\ Di\ \rho} \tag{6}$$

For two-phase flow, the mechanical energy balance requires some modifications, the insertion of the two-phase density ($\rho_{tp}$) in the kinetic term, and the introduction of the two-phase pressure drop enhancement factor ($\varphi^2_{lo}$), calculated using the methods described in Smith [6]:

$$-\frac{dP}{dL} = -\frac{G^2}{\rho_{tp}^2}\frac{d\rho_{tp}}{dL} + \rho_{tp}\ g\ sen\theta + \varphi_{lo}^2 \frac{f\ G^2}{2\ Di\ \rho} \tag{7}$$

The mass balances in the two-phase regions describe the flow rate of each phase, represented by the two algebraic equations

$$mT = mV + mL \tag{8}$$

$$mV = \left(\frac{\mathcal{V} MMmg}{\mathcal{V} MMmg + (1-\mathcal{V}) MMml}\right) mT \tag{9}$$

The composition of each phase along the model integration is evaluated using a flash calculation routine according to Smith et al. [8]. The gas phase is assumed ideal and the liquid phase thermodynamic behaviour is described using the Wilson model of activity coefficient.

The thermofluidynamic properties of each phase (density, heat capacity, viscosity, thermal conductivity, and the surface tension) are calculated using correlations described in Reid et al., and Faghri and Zhang [7,8].

## SIMULATION

The system flow rate must consider the hydraulic balance along the entire flow circuit. Therefore, the mass flow rate is calculated using a convergence loop, as shown in Figure 2, using the Regula-Falsi method.

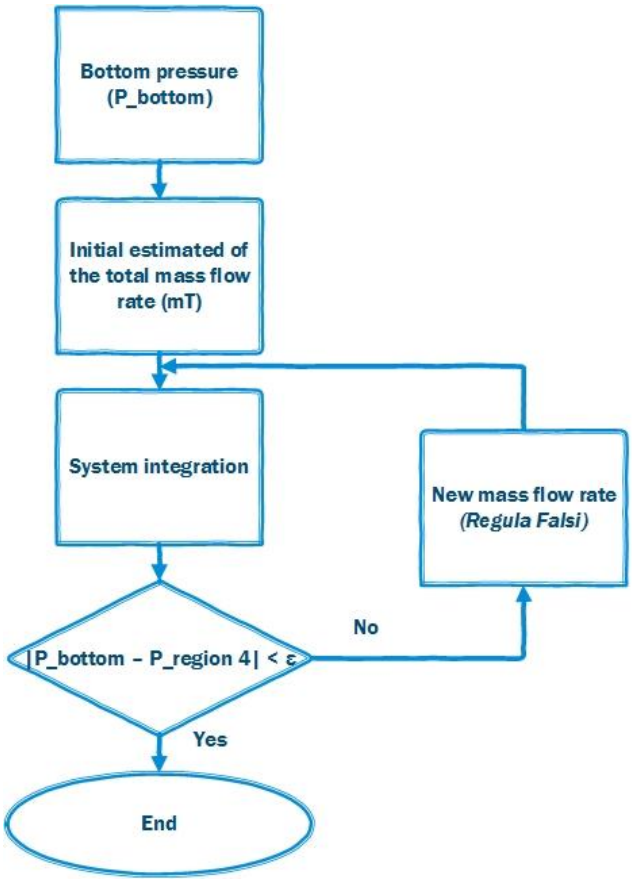


**Figure 2** Mass flow rate convergence loop

The simulation involves the sequential integration of the model equations along each region.

The simulation of Region 1 consists in the integration of the flow equation (Equation 6) from the liquid surface in the tower bottom until the heat exchanger inlet. The temperature is assumed constant along this region.

Region 2 is simulated through the integration of the energy and flow equations, without bulk phase change (Equations 1 to 6). This region ends when the saturated conditions are reached according to the stream bulk temperature and pressure.

Region 3 simulation encompasses the integration of energy, flow and mass balances (Equations 1 to 5 and 7 to 9) along the two-phase flow inside the heat exchanger.

Finally, the simulation of Region 4 is similar to the Region 3, without the term associated to the heat transfer (the return line is considered perfectly insulated).

The numerical integration is conducted using the code DASSL, present in the Scilab software.

## RESULTS

In order to illustrate the use of the algorithm developed, it was proposed an example of the vaporization of a binary mixture with 20 % acetone and 80 % water (molar basis). Table 1 shows the system configuration, according to the circuit lengths depicted in Figure 1, Table 2 presents the details of the thermal service, and Table 3 shows the mechanical data of the heat exchanger.

**Table 1** – System configuration

| | |
|---|---|
| **Length of the Region 1** | |
| L1 (m) | 2.0 |
| L2 (m) | 2.0 |
| L3 (m) | 1.5 |
| **Length of the Regions 2 and 3** | |
| L_heating + L_vaporization (m) | 1.2 |
| **Length of the Region 4** | |
| L4 (m) | 0.96 |

**Table 2** – Thermal service

| | | |
|---|---|---|
| **Tube side** | Inlet pressure (kPa) | 164.4 |
| | Fouling resistance (m² K/W) | 0.00053 |
| **Shell side** | Fluid | Saturated steam |
| | Inlet temperature (K) | 460 |
| | Fouling resistance (m² K/W) | 0.000088 |

**Table 3** – Mechanical data of the heat exchanger

| | |
|---|---|
| Length of tubes (m) | 1.2 |
| Number of tubes | 29 |
| Inner tube diameter (m) | 0.02622 |
| Outer tube diameter (m) | 0.03175 |

The simulation of the termosiphon system determines a total mass flow rate of 14.16 kg/s. The heat load of the reboiler is 621.5 kW. The vapor fraction in the exchanger outlet is 6.73 %, which complies with the limits specified for water and aqueous solutions of 2 % to 10 % [3].

Figures 3 to 6 shows the pressure, temperature, vapor and liquid mass flow rates according to each region.

Figure 3a shows the profile of the pressure along the Region 1. In this graph, it can be seen that up to 2 meters, the pressure increases due to the downward flow in the region where the conversion of potential energy into pressure energy occurs. Between 2 and 4 meters, the pressure is approximately constant, because the flow is horizontal in this part of the region. The final 1.5 meters (4 to 5.5 m), the pressure falls, because of the upflow. The other variables shown in Figures 3b, 3c, and 3d remain constant, since it is assumed that there is only pressure variation in this region.

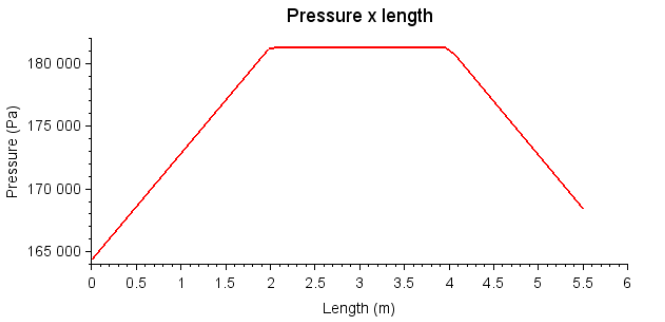


(a)

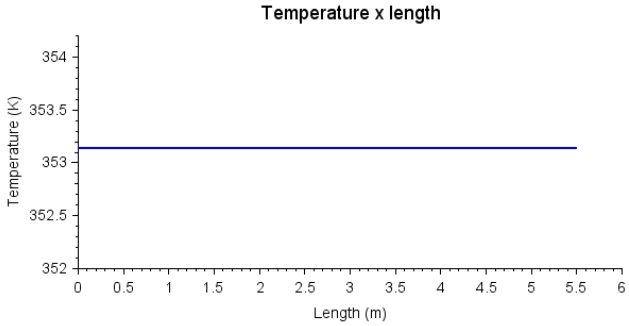


(b)

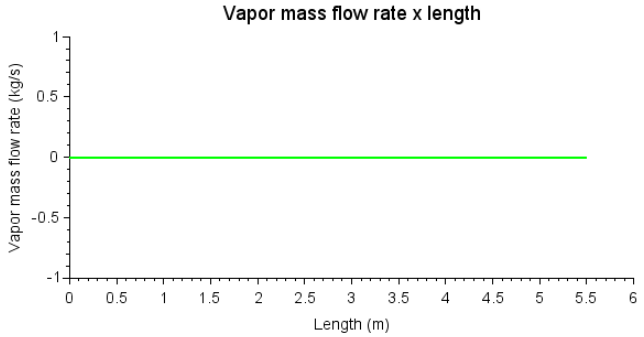


(c)

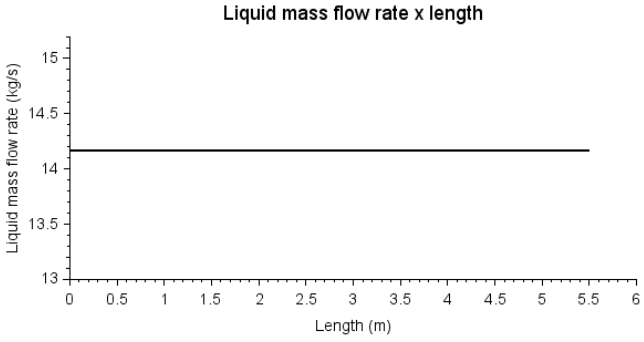


(d)

**Figure 3** Pressure, temperature, vapor mass flow rate and liquid mass flow rate profiles in Region 1.

Region 2 is characterized by heating the fluid before the vaporization, so the vapor and liquid flow rates are also unchanged. Figure 4a shows the decrease of the pressure due to the upflow and head loss. The temperature variation due to the heat transfer is depicted in Figure 4b. Figures 4c and 4d show the constant profiles of the liquid and vapor mass flow rates.

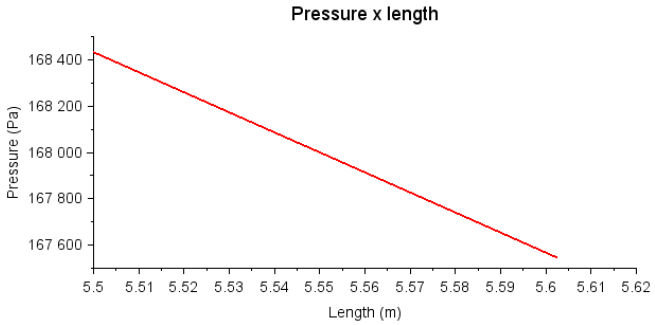


(a)

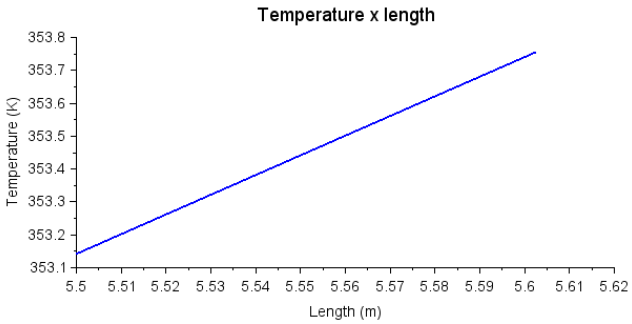


(b)

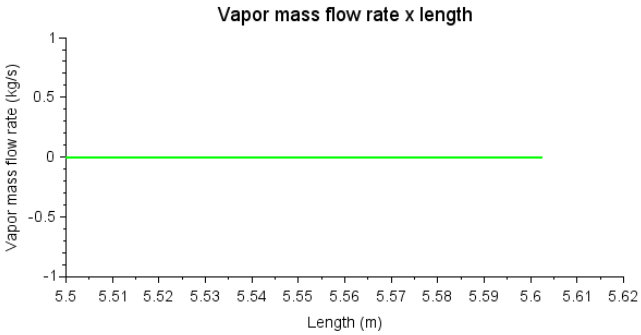


(c)

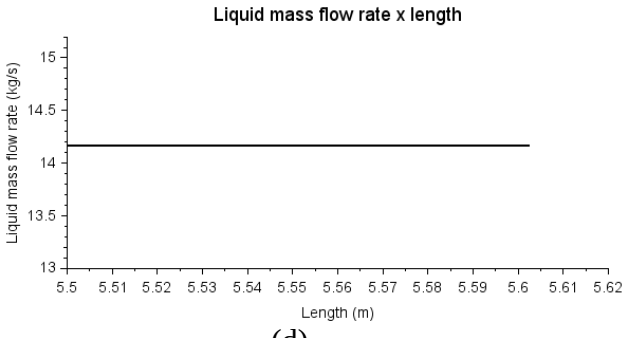


(d)

**Figure 4** Pressure, temperature, vapor mass flow rate and liquid mass flow rate profiles in Region 2.

In Region 3, it is observed a further reduction of the pressure because of the upward flow and head loss, as shown in Figure 5a. Despite the heating, the temperature variation in Figure 4b occurs associated to the pressure decrease, i.e. the reduction of the pressure tends to decrease the saturation temperature. Figure 5c and Figure 5d show the increase of the vapor flow rate and the decrease of the liquid flow rate due to the vaporization.

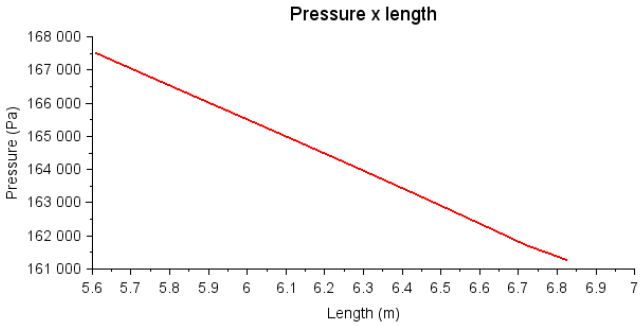


(a)

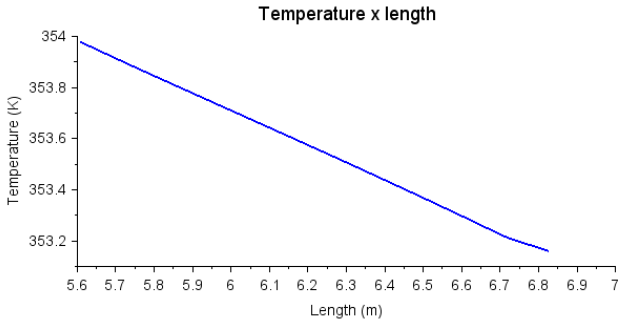


(b)

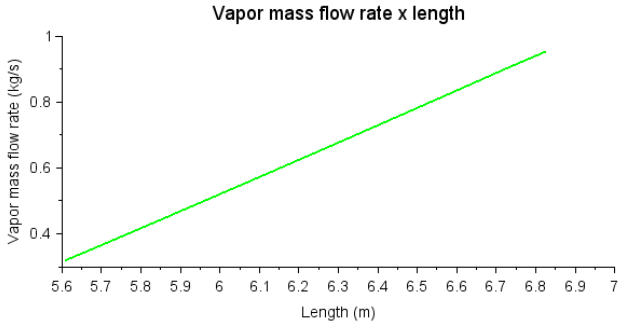


(c)

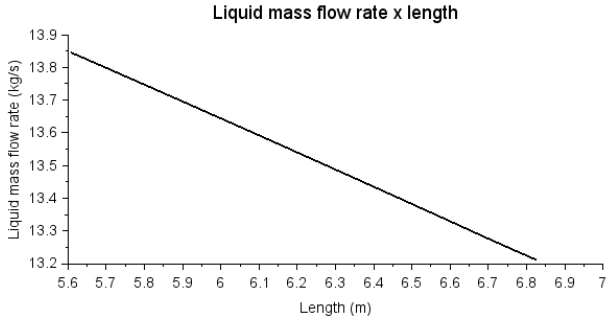


(d)

**Figure 5** Pressure, temperature, vapor mass flow rate and liquid mass flow rate profiles in Region 3.

Region 4 is characterized by a reduction in the pressure associated with the head loss of the two-phase flow, as depicted in Figure 6a. As a consequence, the temperature drops approximately 0.15 K associated with the pressure change in this region, as shown in Figure 6b. The variations observed in Figures 6c and 6d are related to the small vaporization that occurs in this region.

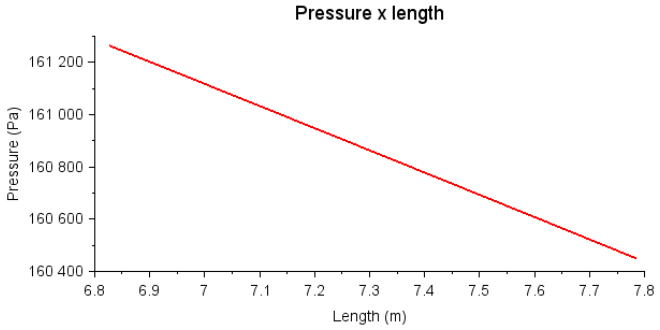


(a)

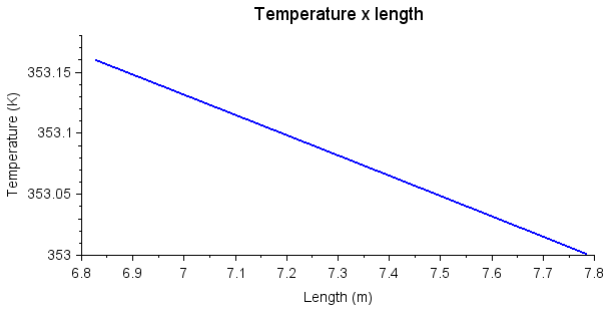


(b)

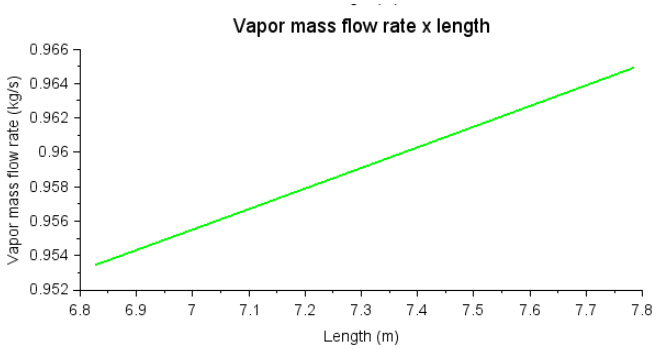


(c)

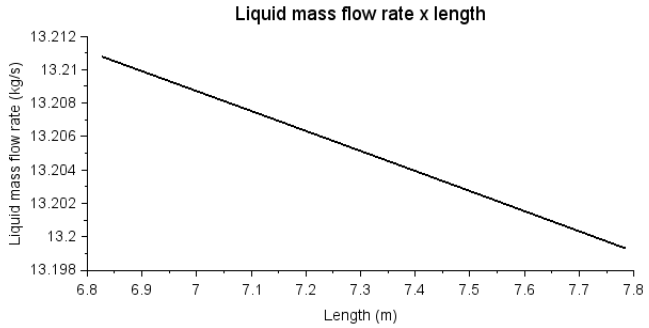


(d)

**Figure 6** Pressure, temperature, vapor mass flow rate and liquid mass flow rate profiles in Region 4.

## CONCLUSION

The modelling and simulation of reboilers is a very important tool for the design of such equipment, which are of great importance in the chemical industry. This study aimed to present a model for vertical thermosiphons, using a system of differential algebraic equations. The results obtained in a simulation example are consistent with the expected behaviour for such thermohydraulic circuits.

## REFERENCES

[1] Arneth, S.; Stichlmair, J., Characteristics of thermosiphon reboilers, *International Journal of Thermal Sciences*, Vol. 40, 2001, pp. 385–391.

[2] Serth, R.W., Lestina, T., *Process Heat Transfer: Principles, Applications and Rules of Thumb.* 2nd ed., Elsevier, 2014.

[3] Palen, J.W. Shell and tube reboilers, in *Heat Exchanger Design Handbook. Hemisphere*, v. 3, Hemisphere Publishing, 1983

[4] Incropera, F.P.;De Witt, D.P.; Bergman, T.L.; Lavine, A.S. *Fundamentals of Heat and Mass Transfer*, 6th Ed., John Wiley & Sons Inc., 2007.

[5] Smith, R.A. *Vaporisers: Selection, Design and Operation.* Longman Scientific and Technical, UK, 1986

[6] Smith, J.M.; Van Ness, H.C.; Abbott, M.M. *Introduction to Chemical Engineering Thermodynamics*, 7th ed., McGraw-Hill Education, 2004.

[7] Reid, R.C., Prausnitz, J.M., Poling, B.E., *The Properties of Gases and Liquids*, 4th ed. New York: McGraw-Hill, 1987.

[8] Faghri, A.; Zhang, Y., *Transport Phenomena in Multiphase Systems*. 1st ed. Amsterdam: Elsevier, 2006.